

# Skin-Friction and Forced Convection from Rough and Smooth Plates

Aubrey G. Jaffer  
e-mail: agj@alum.mit.edu

## Abstract

The current models for skin-friction drag from a plate with a rough surface are derived by analogy to flow within pipes having rough interiors. But this analogy fails at low Reynolds number (Re) flow rates because the boundary-layer must compress into the center of the pipe, while the plate boundary-layer is unbounded. A significant discrepancy from the pipe analogy at low Re was found by the rough plate experiments of Pimenta, Moffat, and Kays (1975) and by experiments conducted by the present author (2019).

An additional problem is that the roughness parameter in pipe analogy theories is tied to the drag measurements of flows inside Nikuradse’s assortment of sand-roughened pipes (1933). Prandtl and Schlichting (1934) caution that their theory applies only to sand-roughness. More useful would be a theory based on direct measurements of roughness profiles.

The present work derives the formula for a plate’s skin-friction drag coefficient given its root-mean-squared height-of-roughness, and Re bounds from the roughness spatial frequency spectrum.

The present theory is in close agreement with the Mills-Hang (1983) theory, the Pimenta et al measurements, and the experiments conducted by the author over their respective Re ranges.

From boundary conditions of its rough plate analysis, the present work also derives an exact formula for skin-friction from a smooth plate; this formula is in very close agreement with measurements from Smith and Walker (1959) and Spalding and Chi (1964) over 4 decades of Re.

**Keywords:** rough turbulence; profile roughness; skin-friction; forced-convection

This research did not receive any specific grant from funding agencies in the public, commercial, or not-for-profit sectors.

## Table of contents

1. <i>Introduction</i> .....	2
2. <i>Prior work</i> .....	3
3. <i>Rough turbulence</i> .....	4
4. <i>Roughness</i> .....	4
5. <i>Self-similar profile roughness</i> .....	5
6. <i>Roughness travel</i> .....	6
7. <i>Skin-friction</i> .....	7
8. <i>Spectral roughness</i> .....	9
9. <i>Periodic roughness</i> .....	10
10. <i>Periodic smoothness</i> .....	12
11. <i>Local skin-friction</i> .....	13
12. <i>Forced convection</i> .....	13
13. <i>Experimental results</i> .....	14
14. <i>Fully rough regime</i> .....	15
15. <i>Transitional rough regime</i> .....	16
16. <i>Discussion</i> .....	17
17. <i>Conclusions</i> .....	18
18. <i>Nomenclature</i> .....	19
19. <i>References</i> .....	20

## 1. Introduction

Skin-friction drag is the pressure opposing a flow due to viscous dissipation of the turbulence generated by that flow along a surface. Skin-friction drag is important to the fluid dynamics of vehicles and turbines. The related phenomenon of forced convection has application to modeling weather and the thermal behavior of buildings.

In 1934 Prandtl and Schlichting published *Das Widerstandsgesetz rauher Platten (The Resistance Law for Rough Plates [1])*, which brilliantly infers a relation for skin-friction resistance for rough plates from their analysis of Nikuradse’s measurements of sand glued inside pipes (“sand-roughness”). At the conclusion of the paper they write:

“The resistance law just derived for rough plates has chiefly validity for a very specific type of roughness, namely a smooth surface to which sand grains have been densely attached and where the Nikuradse pipe results have been taken as the basis. . . .

A single roughness parameter (the relative roughness) will in all likelihood no longer answer the purpose in continued investigations of the roughness problem.”

Hama [2] lays out three challenges to the pipe-plate analogy:

“Now there is no obvious reason why pipe flow and boundary-layer flow should be identical or even similar. First, a pressure gradient is essential for flow through a pipe but not along a plate. Second, pipe flow is confined and perforce uniform, while flow along a plate develops semi-freely and bears no such a priori guarantee of displaying similar velocity profiles at successive sections. Finally, the diameter and roughness size are the only geometrical dimensions of established flow in pipes, whereas at least three linear quantities are necessary to characterize the boundary layer.”

Hama attempts to confirm the pipe-plate analogy with measurements of wire screens affixed to flat plates, but concludes that confirmation is uncertain for all but large Reynolds numbers ( $Re$ ).

The roughness in prior works [1] [2] [3] [4] is reported in Nikuradse’s sand-roughness metric  $k_S$ , the height of “coarse and tightly placed roughness elements such as for example coarse sand grains glued on the surface”.

A machined analog to sand-roughness, the plate tested by Pimenta, Moffat, and Kays [3] was composed of 11 layers of densely packed metal balls 1.27 mm in diameter “arranged such that the surface has a regular array of hemispherical roughness elements.” Pimenta et al write that, while the agreement of their data with the Prandtl-Schlichting plate model is “rather good” in the fully rough regime, their apparatus does not have the same behavior as “Nikuradse’s sand-grain pipe flows in the transition region”.

By taking the wake component of the velocity profile into account, Mills and Hang [4] created a model which improved the match to the Pimenta et al data at large  $Re$ , but did not address the discrepancy for low  $Re$  flows.

The “fully rough regime” refers to a mode of flow in pipes with rough interiors which has larger skin-friction coefficients than similar flow inside smooth pipes. For sand-roughness, the fully rough regime holds at flow rates larger than a transition value; and skin-friction coefficients are insensitive to flow rates larger than that transition value. This behavior for sphere-roughened plates is supported by the measurements from Pimenta et al, but not by the bi-level plates tested by the present author. And at slower flow rates, Hama’s challenges remain unresolved.

These difficulties motivate a new theoretical analysis of flow along plate roughness.

## 2. Prior work

The pipe analogy having some success in the fully rough regime (large  $Re$ ), there are several formulas to compare with those to be developed in the present work.

In *Boundary-layer theory* [5] Prandtl and Schlichting give formulas for fully rough (large  $Re$ ) local ( $c'_f$ ) and average ( $c_f$ ) skin-friction coefficient for a rough flat plate in terms of its sand-roughness  $k_S$  and the distance  $x$  along the plate in the direction of flow up to its characteristic-length  $L$ :

$$c'_f = \left( 2.87 + 1.58 \log_{10} \frac{x}{k_S} \right)^{-2.5} \quad x \leq L \quad (1)$$

$$c_f = \left( 1.89 + 1.62 \log_{10} \frac{L}{k_S} \right)^{-2.5} \quad 10^2 < \frac{L}{k_S} < 10^6 \quad (2)$$

Mills and Hang [4] present a formula (3) which is more accurate than the Prandtl-Schlichting formula (1) on the local skin-friction coefficient measurements from Pimenta et al [3]. Their local and average skin-friction coefficient formulas are:

$$C_f = \left( 3.476 + 0.707 \ln \frac{x}{k_S} \right)^{-2.46} \quad x \leq L \quad (3)$$

$$C_D = \left( 2.635 + 0.618 \ln \frac{L}{k_S} \right)^{-2.57} \quad 750 < \frac{L}{k_S} < 2750 \quad (4)$$

White [6] gives a formula for fully rough local (not average) skin-friction coefficient:

$$C_f = \left( 1.4 + 3.7 \log_{10} \frac{x}{k_S} \right)^{-2} \quad \frac{x}{k_S} > \frac{Re_x}{1000} \Rightarrow \frac{L}{k_S} > \frac{Re}{1000} \quad (5)$$

Prandtl and Schlichting [1], and Mills and Hang [4] both derived the average formulas (2) and (4) respectively from the local formulas by fitting curves to the results of numerical integration:

$$C_D \left( \frac{L}{k_S} \right) = \frac{k_S}{L - L_P} \int_{L_P/k_S}^{L/k_S} C_f(x) dx \quad (6)$$

But the local formulas have a singularity at  $x/k_S = 0$  and can go negative when  $0 < x/k_S < 1$ . The lower limit of integration should be greater than or equal to 1, but is not revealed in their papers. The average formulas are quite sensitive to the lower limit because the largest value of the local formulas occurs there, a region for which  $x/k_S \gg 1$  does not apply.

For the Prandtl-Schlichting formula (1), with a lower bound of 1 (and initial  $dx/k_S = 2$ ), integration of the local  $c'_f$  is within  $\pm 0.5\%$  of the average  $c_f$  in formula (2) over the range  $200 < x/k_S < 200000$ .

For the Mills-Hang formula (3), with a lower bound of 1.6 (and initial  $dx/k_S = 0.01$ ), integration of the local  $C_f$  is within  $\pm 0.5\%$  of the average  $C_D$  in formula (4) over the range  $200 < x/k_S < 200000$ .

Churchill [7] compares eight formulas from various sources with the data from Pimenta et al [3] and doesn't find any to be superior to the Mills-Hang formula (3). It does, however, have different methods for computing the average (mean) skin-friction  $C_m$  from local  $C_f$  for smooth and rough surfaces respectively:

$$C_m = C_f \frac{1 - 4.516\sqrt{C_f}}{1 - 7.965\sqrt{C_f} + 21.52 C_f} \quad C_m = C_f \frac{1 - 4.516\sqrt{C_f}}{1 - 7.965\sqrt{C_f}} \quad (7)$$

Prandtl and Schlichting [1], and Mills and Hang [4] incorrectly applied smooth plate averaging (6) to rough plates, but had no average measured data to compare with.

The utility of all of the formulas would be much greater if they were defined in terms of a roughness metric applicable to any surface. The most commonly used traceable roughness metrics are root-mean-squared (RMS) and arithmetic-mean height-of-roughness.

Afzal, Seena, and Bushra [8] fit 5.333 for the RMS to sand-roughness conversion factor and 6.45 for arithmetic-mean to sand-roughness in pipes.

Flack, Schultz, Barros, and Kim [9] measured skin-friction from grit-blasted surfaces in a duct. They write "The root-mean-square roughness height ( $k_{rms}$ ) is shown to be most strongly correlated with the equivalent sand-roughness height ( $k_S$ ) for the grit-blasted surfaces."

### 3. Rough turbulence

Forced flow along a flat plate with a rough surface is different in character from forced flow along a smooth surface because the peaks of roughness protrude through what would otherwise be a viscous sub-layer adjacent to the plate. Lienhard and Lienhard [10] teach: “Even a small wall roughness can disrupt this thin sublayer, causing a large decrease in the thermal resistance (but also a large increase in the wall shear stress).”

If boundary-layers are disrupted by roughness, then it is better to consider the effect of roughness on flow as a series of disruptions than as a continuous boundary-layer. The present work takes this approach.

In order to guarantee that the turbulence generated by flow along a rough surface is rough turbulent, there should be disruptive roughness along the whole length of the flow over the plate. The turbulent boundary-layer depth along a smooth plate increases as  $x^{4/5}$ , where  $x$  is the distance from its leading edge. Roughness whose envelope height increases linearly with  $x$  can disrupt a smooth boundary layer repeatedly along the whole plate.

Although vortexes can arise in two-dimensional systems, turbulence is a three-dimensional phenomena. Its random velocity fluctuations must be isotropic at all but the coarsest length scales. In order that the turbulence velocity differences from the bulk flow resulting from interactions with the plate roughness are evenly distributed, the roughness should be at least weakly isotropic; rotating the plate should not substantially affect the behavior of the system. A plate surface composed of parallel ridges and valleys would not meet this criterion.

### 4. Roughness

Let “profile roughness” be a function  $z(x)$  where  $0 \leq x \leq L$  is distance from the leading edge in the direction of flow. Functions being single-valued, neither tunnels nor overhangs are allowed.

Consider the roughness profile  $z(x)$ . Its mean height  $\bar{z}$  and root-mean-squared height-of-roughness  $\epsilon$  are:

$$\bar{z} = \frac{1}{L} \int_0^L z(x) dx \quad \epsilon = \sqrt{\frac{1}{L} \int_0^L [z(x) - \bar{z}]^2 dx} \quad (8)$$

The roughness function  $z(x)$  need not be continuous to be integrable. So local flow properties may not be well-defined anywhere. For these reasons, the present analysis focuses on the average skin-friction coefficient  $f_C$ .

A profile roughness function  $z(x)$  has “self-similar roughness” with (integer) branching factor  $n \geq 2$  if the RMS height-of-roughness of  $z(x)$  over an interval  $x_0 < x < x_n$  is  $n$  times the RMS height-of-roughness of  $z(x)$  over each (evenly divided) sub-interval  $x_\iota < x < x_{\iota+1}$  for  $0 \leq \iota < n$  at a succession of scales converging to zero.<sup>1</sup> A consequence of this definition of self-similar roughness is that the ratio of the length of the interval  $L = x_n - x_0$  to its RMS height-of-roughness  $\epsilon$  will be invariant over its succession of scales.

Self-similarity is of interest because the average skin-friction coefficient  $f_C$  is a function of  $L/\epsilon$ . If the roughness is self-similar, then  $L/\epsilon$  and  $f_C(L/\epsilon)$  will be constant over the span of the roughness profile.

Of particular interest are self-similar roughness profiles that are permutations of the linear ramp  $z(x) = x$  from  $x = 0$  to  $x = w$ . Every elevation from 0 to  $w$  occurs exactly once in a ramp-permutation. Because the RMS height-of-roughness calculation depends only on the  $z$  values and not their relation to  $x$ , for all ramp-permutation profile roughness:

$$\epsilon = \sqrt{\frac{1}{w} \int_0^w [x - w/2]^2 dx} = \frac{w}{\sqrt{12}} \quad (9)$$

This raises the question of whether the linear ramp, which is the identity permutation of a linear ramp, can produce rough turbulence from a steady flow. A ramp doesn’t meet the isotropy requirement of Section 3 because a plate with a ramp profile in both directions has 0 profile roughness perpendicular to its gradient.

---

<sup>1</sup> Note that  $z(x_\iota)$  values contribute to the interval height-of-roughness, but not to any sub-interval height-of-roughness.

## 5. Self-similar profile roughness

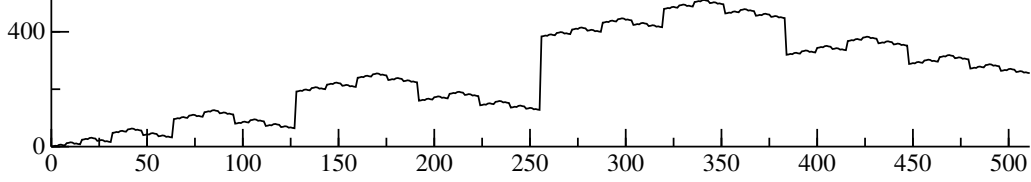


**Figure 1 Gray-code profile roughness**

The integer Gray-code sequence  $G(x, w)$  with  $0 \leq x < w = 2^l$  shown in Figure 1 has an RMS height-of-roughness  $\epsilon = w/\sqrt{12}$  from equation (9) and is a self-similar roughness (bisected;  $n = 2$ ) as seen by its recurrence:

$$G(x, w) = \begin{cases} x, & \text{if } w = 1; \\ w + G(w - 1 - (x \bmod w), w/2), & \text{if } \lfloor x/w \rfloor = 1; \\ G(x \bmod w, w/2), & \text{otherwise.} \end{cases} \quad (10)$$

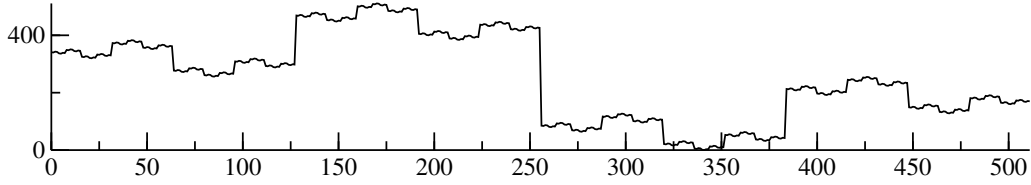


**Figure 2 Wiggliest self-similar profile roughness**

The integer sequence  $W(x, w)$ , which reverses direction at each bifurcation, produces the wiggliest possible self-similar roughness with  $0 \leq x < w = 2^l$  and is shown in Figure 2. Being a ramp-permutation, it has an RMS height-of-roughness  $\epsilon = w/\sqrt{12}$ :

$$W(x, w) = \begin{cases} x, & \text{if } w = 1; \\ \lfloor x/w \rfloor w + W(w - 1 - (x \bmod w), w/2), & \text{otherwise.} \end{cases} \quad (11)$$

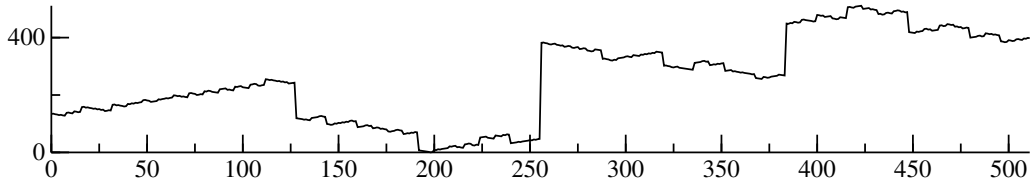


**Figure 3 Randomly reversing bifurcation profile roughness**

Figure 3 shows an integer sequence generated by recursive-descent with random reversing at each bifurcation. Being a ramp-permutation, it has an RMS height-of-roughness  $\epsilon = w/\sqrt{12}$ ; its roughness is approximately self-similar.

There are  $2^w$  distinct self-similar ramp-permutation roughness profiles. Profiles chosen randomly have  $w$  bits of sequence entropy ( $w/2$  bits of Shannon entropy). There are only two distinct ramp profiles and only two distinct wiggliest profiles; their sequence entropies are 1 bit.

## 6. Roughness travel

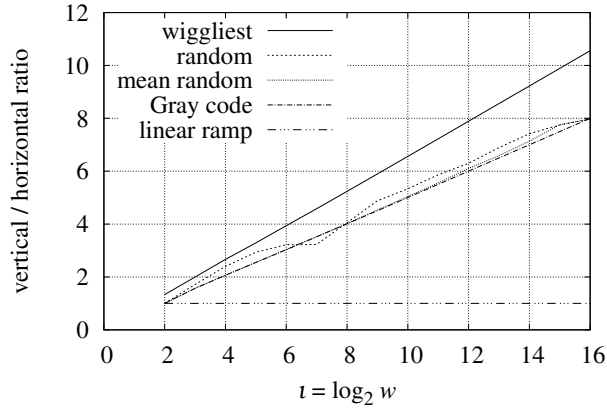


**Figure 4** Travel along profile roughness

In order to convert some of the flow to rough turbulence, parcels of fluid must move in directions not parallel to the bulk flow. Such movement would result from deflection of flow by the vertical spans of discrete profile roughness; the amount of turbulence produced would grow with the height-of-roughness.

For integer ramp-permutation roughness profile  $Y(x, w)$ , the sum of the lengths of all horizontal segments is  $w - 1 = 2^\iota - 1$ . The sum of the absolute value of the length of each vertical segment is:

$$\sum_{x=0}^{2^\iota-2} |Y(x, 2^\iota) - Y(x+1, 2^\iota)| \quad (12)$$

If a parcel of fluid were to trace the ramp-permutation roughness profile  $Y(x, w)$  from  $x = 0$  to  $x = w - 1$ , then  $w - 1$  is the horizontal distance it would travel, while formula (12) is the vertical distance.

Shown in Figure 4 is the vertical to horizontal travel ratio versus  $\iota$ , the base-2 logarithm of  $w$ . The slope is 1/2 for the Gray-code and random-reversal cases, 0 for the linear ramp, and 2/3 for the wiggliest roughness  $W$ . The vertical segments in Figure 2 are indeed longer than the vertical segments in Figures 1 and 3.

A wiggliest roughness profile  $W(x, w)$  is an extreme case; it reverses vertical direction at each increment of  $x$ . For each wiggliest roughness profile there are many more random bifurcation roughness profiles. Going forward,  $W(x, w)$  will be excluded as an outlier.

From Figure 4, the vertical to horizontal travel ratio for the Gray-code and random-reversal sequences deviates little from:

$$\frac{\iota}{2} = \frac{\log_2 w}{2} \quad (13)$$

Formula (13) needs to be normalized by the height-of-roughness  $\epsilon$ . Turning to dimensional analysis, the argument to  $\log_2$  must be dimensionless, involve  $\epsilon$ , and be greater than 1 so that the logarithm is positive. Replacing  $w$  with  $L/\epsilon$ , the ratio of vertical to horizontal travel is then:

$$\frac{2}{\log_2(L/\epsilon)} \quad (14)$$

From equation (9), the maximum peak-to-valley height is  $\sqrt{12}$  times the RMS height-of-roughness  $\epsilon$ . So the vertical to horizontal ratio should be scaled:

$$\frac{1}{\sqrt{12}} \frac{2}{\log_2(L/\epsilon)} = \frac{1}{\sqrt{3} \log_2(L/\epsilon)} \quad (15)$$

Newberry and Savage [11] demonstrate that some self-similar systems which are modeled using continuous power-law probability distributions (such as the Pareto distribution) are better modeled using discrete power-law distributions.

The present work uses their idea in reverse. Conversion of flow into turbulence by contact with discrete self-similar roughness having been modeled above, the turbulence generation by a random self-similar roughness will be inferred using a random variable.

The base-2 logarithm is an artifact of the discrete roughness functions from Section 5. The analogous mean field theory is to treat  $Z = |\Delta Y|$  as a continuous random variable having a Pareto distribution where the frequency of  $Z$  is inversely proportional to  $Z^2$ :

$$1 \left/ \left[ \int_{\epsilon}^L \frac{\sqrt{3} Z}{Z^2} dZ \right] \right. = \frac{1}{\sqrt{3} \ln(L/\epsilon)} \quad (16)$$

In this generalization of formula (15) to isotropic self-similar roughness, the surface height-of-roughness  $\epsilon$ , defined in (17), is used in formula (16) instead of the profile height-of-roughness  $\epsilon$ .

$$\bar{z} = \frac{1}{A} \int_A z dA \quad \epsilon = \sqrt{\frac{1}{A} \int_A [z - \bar{z}]^2 dA} \quad (17)$$

Note that  $\epsilon(Y \times Y) = \sqrt{2} \epsilon(Y)$ . However, the average path length a parcel takes through  $Y \times Y$  is similarly increased. So the ratio of  $L$  to height-of-roughness remains the same.

## 7. Skin-friction

For a rough flat surface subjected to a steady flow parallel to its surface which is sufficiently fast to generate rough turbulence, the skin-friction drag is the pressure opposing the flow due to viscous dissipation of that turbulence.

The skin-friction coefficient  $f_C$  is the ratio of the shear stress  $\tau$ , which is primarily the skin-friction drag when  $L/\epsilon \gg 1$ , to the flow's kinetic energy density  $\rho v^2/2$ , where  $v$  is the bulk flow velocity and  $\rho$  is the fluid density.

$$f_C = \frac{\tau}{\rho v^2/2} \quad (18)$$

$f_C$  is dimensionless; both  $\tau$  and  $\rho v^2/2$  have units of pressure,  $\text{kg}/(\text{m} \cdot \text{s}^2)$ .

Scaling by the vertical to horizontal travel ratio from formula (16) converts a horizontal velocity  $v$  to a friction velocity  $v^*$ , from which  $\tau$  is derived:<sup>2</sup>

$$v^* = \frac{v}{\sqrt{3} \ln(L/\epsilon)} \quad \tau = \frac{\rho v^{*2}}{2} = \frac{\rho v^2}{6 \ln^2(L/\epsilon)} \quad \frac{L}{\epsilon} \gg 1 \quad (19)$$

Combining equations (18) and (19) produces a formula for  $f_C$  dependent only on  $L/\epsilon$ :

$$f_C = \frac{1}{3 \ln^2(L/\epsilon)} \quad \frac{L}{\epsilon} \gg 1 \quad (20)$$

This analysis can be extended to smooth plates. For a given  $\text{Re}$  there must be some roughness ratio  $L/\epsilon$  so large that it behaves as a smooth surface rather than a rough surface. The roughness Reynolds number  $\text{Re}_\epsilon$  is the dimensionless friction velocity with characteristic-length  $L$ :

$$\text{Re}_\epsilon = \frac{v^* \epsilon}{\nu} = \frac{v}{\sqrt{3} \ln(L/\epsilon)} \frac{\epsilon}{\nu} = \frac{\text{Re}}{\sqrt{3} [L/\epsilon] \ln(L/\epsilon)} \quad (21)$$

The  $\text{Re}$  at which the skin-friction from the rough plate transitions to the skin-friction from a smooth plate will have the same  $\text{Re}_\epsilon$  value at all  $L/\epsilon \gg 1$  scales. Combining formula (21) with  $\text{Re}_\epsilon = 1$  relates  $\text{Re}$  to  $L/\epsilon$  at transition:

$$\text{Re} = \sqrt{3} \frac{L}{\epsilon} \ln \frac{L}{\epsilon} \quad (22)$$

---

<sup>2</sup> Prandtl and Schlichting [1] calculate  $\tau$  as  $\tau = \rho v^{*2}$ , not  $\tau = \rho v^{*2}/2$ . This results in Prandtl-Schlichting  $c_f$  being twice  $f_C$  of the present work.  $f_C$  is scaled correctly for the Chilton-Colburn analogy (47);  $c_f$  is not.

Knowing that the smooth turbulent and rough turbulent skin-friction coefficients are related near the Re transition, and knowing the transition Re relation to  $L/\varepsilon$ , suggests that the smooth turbulent skin-friction coefficient can be inferred from formulas (22) and (20). With the inclusion of two scale factors it can:

$$f_{C\sigma} = \sqrt[3]{2} f_C \left( \frac{L}{e\varepsilon} \right) = \sqrt[3]{2} \left[ \frac{1}{3} \ln^{-2} \frac{L}{e\varepsilon} \right] \quad \text{Re} = \sqrt{3} \frac{L}{\varepsilon} \ln \frac{L}{\varepsilon} \quad (23)$$

Formula (23) can be solved using the Lambert  $W$  function. The inverse of  $y = x \ln x$  is  $x = \exp(W_0(y))$ , where  $W_0$  is the smallest positive branch of the Lambert  $W$  function. Euler's number  $e = \exp(1)$  is a fixed point of  $x \ln x$  and its inverse,  $\exp(W_0(y))$ . Dividing  $L/\varepsilon$  by  $e$  moves the Re lower bound from zero to  $\sqrt{3}e \approx 4.71$ . The coefficient  $\sqrt[3]{2} \approx 1.26$  is related to  $\sqrt[3]{3} \equiv \sqrt{3}$ .

$$f_{C\sigma}(\text{Re}) = \frac{\sqrt[3]{2}}{3} \ln^{-2} \left( \frac{\exp(W_0(\text{Re}/\sqrt{3}))}{e} \right) = \frac{\sqrt[3]{2}/3}{[W_0(\text{Re}/\sqrt{3}) - 1]^2} \quad \text{Re} \gg \sqrt{3}e \quad (24)$$

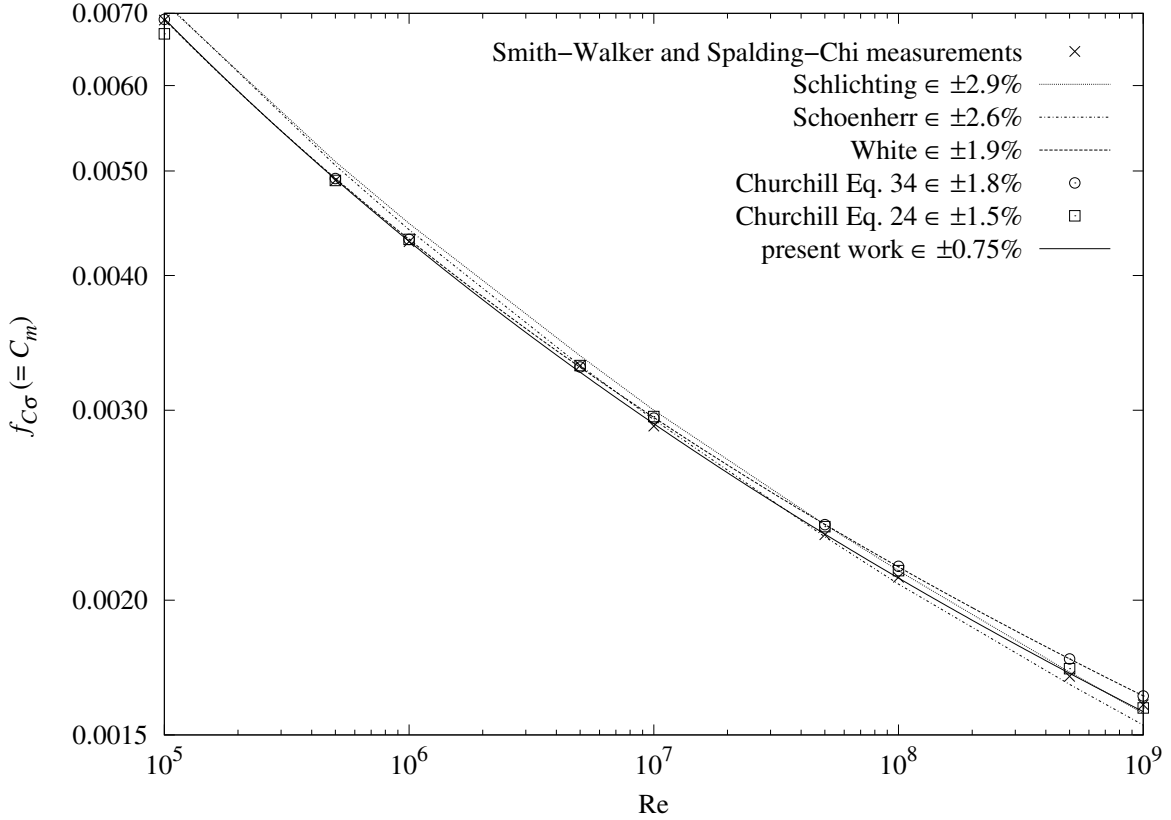


**Figure 5**  $f_{C\sigma}$  versus Re of smooth plate

Churchill [7] compares smooth turbulent formulas from various sources with measured data from Smith and Walker [12], and Spalding and Chi [13]. The data and formula values as digitized by Churchill, and the “present work” smooth turbulence formula (23) are shown in Figure 5. The “present work” formula (23) has 0.75% RMS deviation from the “Smith-Walker and Spalding-Chi measurements”; the second closest is “Churchill Eq. 24” with 1.5%.

Eliminating  $L/\varepsilon$  from formula (23), the implicit equation is:

$$\ln \frac{\text{Re} \sqrt{f_{C\sigma}}}{\sqrt{3} f_{C\sigma} + \sqrt[6]{2}} = \frac{\sqrt{3} f_{C\sigma} + \sqrt[6]{2}}{\sqrt{3} f_{C\sigma}} \quad \text{Re} \gg \sqrt{3}e \quad (25)$$

## 8. Spectral roughness

There is a deep connection between the discrete Fourier transform  $X_j$  of a discrete roughness profile  $Y(x, w)$  and its RMS height-of-roughness  $\epsilon$ :

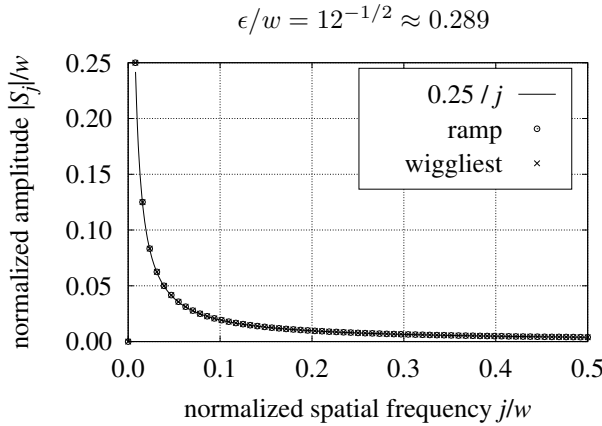
$$X_j = \sum_{x=0}^{w-1} Y(x, w) e^{-2\pi i j x/w} \quad \epsilon = \sqrt{\frac{1}{w} \sum_{j=1}^{w-1} |X_j|^2} \quad (26)$$

Note that the constant term,  $X_0$  (which is the mean value of  $Y$ ), is not included in the sum for  $\epsilon$ .

Because each discrete Fourier coefficient is a Riemann sum over rectangles sampled at their left corners, the discrete Fourier transform underestimates the area under the integrals and introduces a phase shift. The compensated spectrum is:

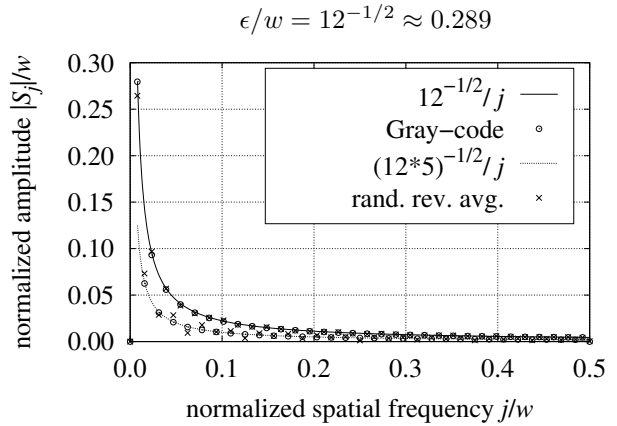
$$S_j = X_j \frac{w}{2j} \sin \frac{\pi j}{w} \exp \frac{\pi i j}{w} \quad 0 < j \leq \frac{w}{2} \quad (27)$$

Because of sampling noise, such compensation is not warranted for physical roughness measurements.



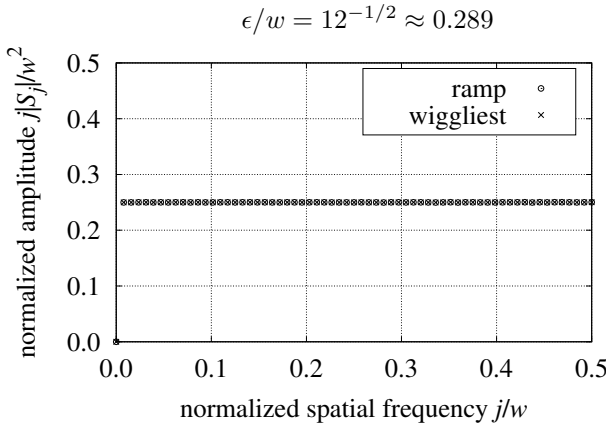
**Figure 6** wiggliest and ramp spectra

Figure 6 shows the  $|S_j|/w$  spectra of the wiggliest (in Figure 2) and ramp profiles. The amplitudes of the wiggliest and ramp spectra are identical; the difference in their profiles is the phase of the complex-valued  $S_j$ ; the ramp phases are all  $90^\circ$  or all  $-90^\circ$ , while the wiggliest phases are an unequal mixture of  $+90^\circ$  and  $-90^\circ$ .



**Figure 7** Gray and random spectra

Figure 7 shows the  $|S_j|/w$  spectrum of the Gray-code roughness profile (from Figure 1) and the average of the amplitudes of the Fourier spectra of 187 instances of 128-point random-bifurcation profiles. The similarity between these spectra indicates that Gray-code roughness is representative of self-similar ramp-permutation roughness. The phases of the Gray-code spectrum are evenly distributed among  $0^\circ$ ,  $180^\circ$ ,  $63.43^\circ$ , and  $116.57^\circ$ .



**Figure 8** wiggliest and ramp spectra

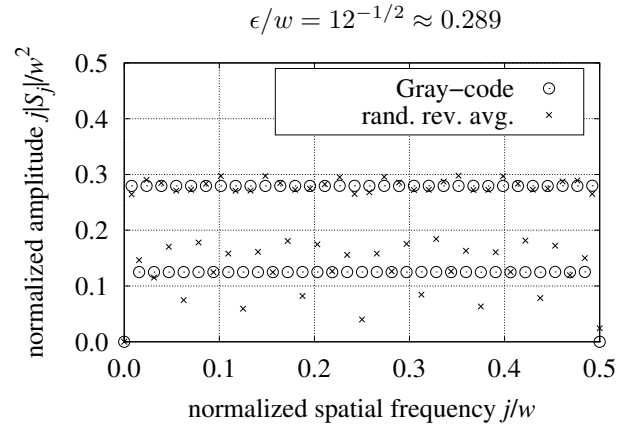


**Figure 9** Gray and random spectra

The similarity length scale is proportional to  $w/j$ . In order to show the spectral structure of roughness across scale,  $j S_j/w^2$  normalizes the spectrum relative to  $S_{j_P}$ , where  $j_P$  is the index of the largest  $|X_j|$ .

Figures 8, 9, and 11 show  $j S_j/w^2$  spectra corresponding to the  $S_j/w$  spectra in Figures 6, 7, and 10 respectively. The traces for the ramp, wiggliest, and Gray-code profiles in Figures 8 and 9 show that these profiles are self-similar; the amplitudes repeat across the spatial frequencies. It is remarkable that the ramp and wiggliest profiles in Figure 8 have identical spectral amplitudes given how differently these two profiles appear. But both are ramp-permutation outliers not covered by the present theory.

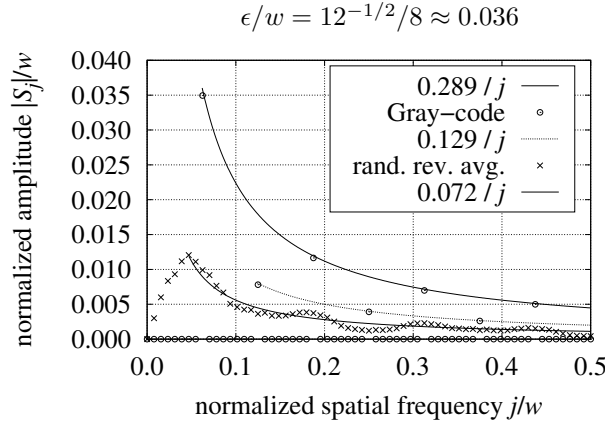


Figure 10 Gray-code eighths spectra

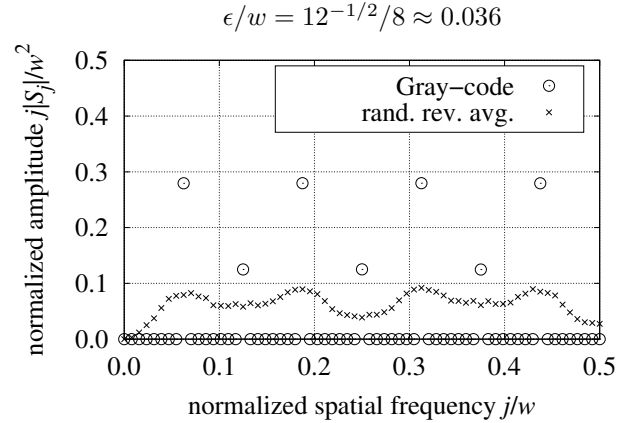


Figure 11 Gray-code eighths spectra

Figure 10 shows spectra of eight concatenated repetitions of a Gray-code profile; and the average of the amplitudes of the Fourier spectra of 187 instances of eight concatenated random reversal profiles. The peak index  $j_P$  of Gray-code eighths is 8 as expected; however the random reversal profiles have  $j_P = 6$  because the amplitudes are not correlated between the random eighths. Figure 11 shows that the random reversal amplitudes are spread compared with the isolated Gray-code amplitudes.

So whether portions are repeated, random, or mixed, the effective period for a roughness profile is  $L_P = L/j_P$ , where  $j_P > 0$  is the index of its largest magnitude discrete Fourier coefficient  $|X_j|$ .

## 9. Periodic roughness

The concept of “uniform roughness” is not compatible with self-similarity; the RMS height-of-roughness of a portion of a self-similar surface must shrink at the succession of scales converging to 0. The existing experimental plates, as well as most manufactured materials consist of repeated patterns of roughness.

Let a plate with “periodic roughness” be a weakly isotropic array of numerous patches, each having approximately the same RMS height-of-roughness  $\varepsilon$ . Each patch can be self-similar or not, as long as they have approximately the same height-of-roughness. From the discrete Fourier transform of the plate’s roughness profile, the effective period  $L_P = L/j_P$ , where  $j_P > 0$  is the index of the  $X_j$  with the largest amplitude.

The sand-roughness described in Section 1 is periodic roughness because the sand grains have uniform size and spacing.

For a periodic roughness with  $0 < \varepsilon < L_P \ll L$  there must be some value of  $Re$  below which the flow exhibits laminar or smooth turbulent behavior along the entire length  $L$  of the plate. The boundary-layer is thinnest at the leading edge. If the boundary layer is going to be disrupted, then it will start within the leading band ( $L_P$ ) of periodic roughness. For this analysis, a boundary layer is considered disrupted when the height-of-roughness of the leading band of the plate is greater than the momentum thickness  $\delta_2$  at local Reynolds number  $Re_x = Re L_P/L$ .

Momentum thickness  $\delta_2$  is not a directly measurable quantity. Schlichting [5] gives the momentum thickness of laminar and smooth turbulent boundary-layers as  $\delta_{2\lambda} = 0.664 x Re_x^{-1/2}$  and  $\delta_{2\sigma} = 0.036 x Re_x^{-1/5}$  respectively. Equivalently, the laminar and smooth turbulent boundary layer thicknesses are:

$$\delta_{2\lambda} = 0.664 \sqrt{Re_x} \frac{L}{Re} \quad \delta_{2\sigma} = 0.036 Re_x^{4/5} \frac{L}{Re} \quad (28)$$

For laminar flow ( $\delta_{2\lambda}$ ), this Blasius boundary-layer model is well supported by measurement. The smooth turbulent  $\delta_{2\sigma}$  formula is less certain. Continuing the analysis of smooth turbulent skin-friction, with free  $\varepsilon$  let  $L/\varepsilon$  be the value producing transition at local Reynolds number  $\text{Re}_x = \text{Re} L_P/L$ . Solving formula (22) for  $L/\varepsilon$ :

$$\frac{L}{\varepsilon} = \exp\left(W_0\left(\frac{\text{Re}_x}{\sqrt{3}}\right)\right) \quad (29)$$

The momentum thickness  $\delta_2$  is proportional to  $L_P$  and the ratio of the friction velocity  $v^*$  in equation (19) to the bulk flow velocity  $v$ :

$$\delta_2 \propto L_P \frac{v^*}{v} = \frac{L_P}{\sqrt{3} \ln L/\varepsilon} = \frac{L_P}{\sqrt{3} W_0(\text{Re}_x/\sqrt{3})} \quad (30)$$

The coefficient seems to be  $1/3^3 \approx 0.0370$ , which may be related to  $\exp(x \ln x) \equiv x^x$ .

$$\delta_2 = \frac{L_P}{3^3} \frac{1}{W_0(\text{Re}_x/\sqrt{3})} \quad (31)$$

Applying the identity  $W_0(x) = x/\exp(W_0(x))$ , formula (32) shows, as with formula (28), that the momentum thickness  $\delta_2$  grows with  $\text{Re}_x$  and shrinks with  $\text{Re}$ :

$$\delta_2 = \frac{L}{3^3} \frac{\exp(W_0(\text{Re}_x/\sqrt{3}))}{(\text{Re}/\sqrt{3})} \quad (32)$$

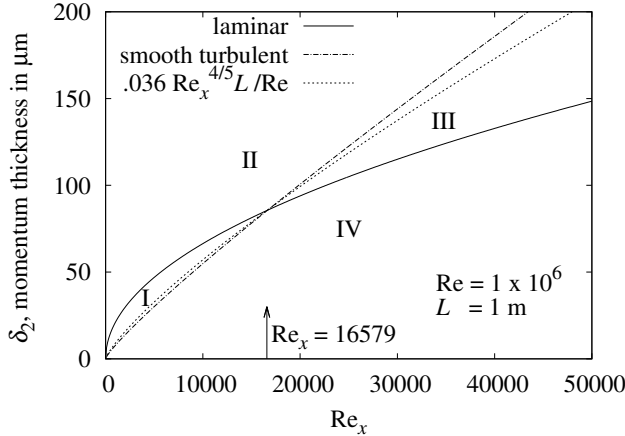


**Figure 12**  $\text{Re}_x$  momentum thickness

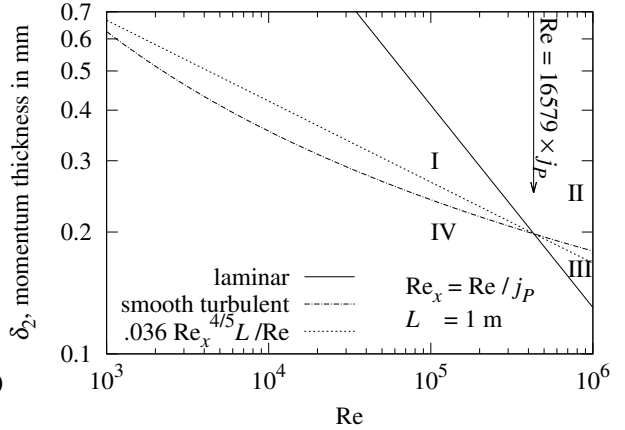


**Figure 13** momentum thickness

Figure 12 and Figure 13 show that “smooth turbulent”  $\delta_2$  from equation (31) and  $\delta_{2\sigma}$  from equation (28) are close at the intersection of the laminar and turbulent curves at:

$$0.664 \sqrt{\text{Re}_x} = 0.036 \text{Re}_x^{4/5} \quad \text{Re}_x = \left(\frac{0.664}{0.036}\right)^{10/3} \approx 16579 \quad (33)$$

Figure 12 shows the theoretical momentum thickness of laminar and smooth turbulent flows over a 1 m long plate with  $\text{Re} = 1 \times 10^6$ . The laminar and turbulent curves divide the graph into four regions. When the point at  $(\text{Re}_x, \varepsilon)$  is in regions I or IV, then it wouldn’t significantly disrupt laminar flow; so the flow over the plate will be laminar. When  $(\text{Re}_x, \varepsilon)$  is in region II, then its height is sufficient to disrupt both laminar and smooth turbulent flow; so the flow over the plate will be rough turbulent.

When  $(\text{Re}_x, \varepsilon)$  is in region III, then the roughness  $\varepsilon$  is sufficient to disrupt laminar flow, but not high enough to disrupt smooth turbulent flow; so the flow over the plate will be smooth turbulent. With  $\delta_{2\lambda} = \varepsilon$  and  $x = L_P$ , solve for the laminar upper-bound  $\text{Re}_\lambda$  and smooth turbulent upper-bound  $\text{Re}_\sigma$ :

$$\text{Re}_\lambda = \left(\frac{0.664}{\varepsilon}\right)^2 L_P L \quad (34)$$

$$\text{Re}_\sigma = \left(\frac{0.036}{\varepsilon}\right)^5 L_P^4 L \quad (35)$$

Equating  $\text{Re}_\lambda$  and  $\text{Re}_\sigma$ :

$$\frac{L_P}{\varepsilon} = \left( \frac{0.664^2}{0.036^5} \right)^{1/3} \approx 193.9 \quad (36)$$

When  $L_P/\varepsilon < 193$ , the flow over the whole plate transitions directly from laminar to rough turbulence at  $\text{Re}_\lambda$ . When  $L_P/\varepsilon > 194$ , then  $\text{Re}_\sigma > \text{Re}_\lambda$  and the flow over the whole plate transitions from laminar to smooth turbulence around  $\text{Re}_\lambda$ , and to rough turbulence around  $\text{Re}_\sigma$ . Lienhard [14] models a gradual transition from laminar to smooth turbulence for smooth plates. But for periodic roughness with  $L_P \ll L$ , the roughness in the leading patch controls the flow over the rest of the plate (which has the same height-of-roughness).

Because the boundary-layer depth shrinks with increasing free-stream velocity, rough turbulence is generally the case for rough plates at large  $\text{Re}$ . Surprisingly, smooth turbulence can also appear at large  $\text{Re}$ .

## 10. Periodic smoothness

In the discussion appended to Hama [2], Dr. S. F. Hoerner points out:

“... there is hardly any physical or natural surface condition which is truly equal or similar to sand roughness. One conclusion from sand experiments has been the expectation that from then on every rough surface should have a constant terminal drag coefficient. As early as 1924, it has been demonstrated (by Hopf and Fromm in *Zeitschr. Angew. Math. Mech.*, 1923:329-339) that certain types of roughness do not show any constant coefficients.”

Consider a smooth flat plate etched with a square grid of narrow grooves which is subjected to a moderate flow parallel to its surface. The boundary-layer near the leading edge will be disrupted by the grooves perpendicular to the flow. If, at the scale of a smooth (square) patch, the smooth turbulent boundary-layer depth at the trailing edge of the patch has a momentum thickness greater than  $2\varepsilon$ , then every patch from that point to the trailing edge of the plate will have smooth turbulent skin-friction  $f_{C\sigma}$ .

Let  $L_T$  be the length of a single patch in the direction of flow. The length variables involved in plate convection are  $L$ ,  $L_T$ ,  $L_P$ ,  $L_P - L_T$ ,  $x$ ,  $\varepsilon$ , and  $\delta_{2\sigma}$ . If the smooth turbulent momentum thickness of the patch is greater than  $2\varepsilon$  and crosses the  $L_P - L_T$  gap, then the downstream flow will be smooth turbulent. Addressing this gap are dimensionless factors forcing the rough turbulence upper-bound  $\text{Re}_\ell$  towards 0 as the gap shrinks.

$$\text{Re}_\ell = \frac{L_P}{L_T} \frac{L_P - L_T}{0.036 L_P} \frac{\varepsilon/4}{L_P - L_T} \frac{L}{0.036 L_P} \left( \frac{2\varepsilon}{0.036 L_P} \right)^{5/4} = \frac{L/8}{0.036 L_T} \left( \frac{2\varepsilon}{0.036 L_P} \right)^{9/4} \quad (37)$$

All surfaces are rough. A patch behaves smoothly if its smooth turbulent boundary-layer isn't disrupted by the roughness  $\varepsilon_q$  of the patch. Treating the patch as a plate with characteristic-length  $L_T$ , period  $L_q$ , and roughness  $\varepsilon_q$ , equation (35) yields  $\text{Re}_\sigma = (L_T/L_q) (0.036 L_q/\varepsilon_q)^5$ . In order for the smooth turbulent boundary-layer to flow over the roughness  $\varepsilon_q$ ,  $\text{Re}_\ell$  must be less than  $\text{Re}_\sigma$  converted to characteristic-length  $L$  by a factor of  $L/L_T$ :

$$\text{Re}_\ell < \frac{L}{L_q} \left( \frac{0.036 L_q}{\varepsilon_q} \right)^5 \quad (38)$$

The local flow transitions from rough to smooth turbulence at  $\text{Re}_x = \text{Re}_\ell$  only when formula (38) is satisfied. Expressing this as a constraint on  $\varepsilon_q$ , smooth turbulence will emerge at  $\text{Re}_x > \text{Re}_\ell$  only if:

$$\varepsilon_q < \frac{L_T}{71.3} \left( \frac{L_T}{L_q} \right)^{0.2} \left( \frac{L_P}{\varepsilon} \right)^{0.45} \quad (39)$$

## 11. Local skin-friction

While the local skin-friction coefficient  $f_c$  is not well defined for self-similar roughness, it is tractable for periodic roughness by avoiding the singularity at the leading edge of the plate. This is done by using  $x_S = L_P/\varepsilon = 5.333 L_P/k_S$  instead of 0 as the lower bound of integration.

The average skin-friction drag  $f_C$  of a continuous boundary-layer is calculated from local drag coefficient  $f_c$  by formula (6), which can be rewritten as:

$$\frac{f_C(x)}{f_c(x)} = \left( \int_{x_S}^x f_c(x) dx / (x - x_S) \right) / f_c(x) \quad (40)$$

But periodic roughness disrupts the boundary layer repeatedly. Instead of  $f_c$  accruing linearly, it should go as the square. This leads to a formula for  $f_C(x)$  given  $f_c(x)$ :

$$\frac{f_C(x)}{f_c(x)} = \left( \left( \int_{x_S}^x f_c(x) dx / (x - x_S) \right) / f_c(x) \right)^2 \quad (41)$$

At  $x/k_S = 750$ , formula (41) has values in excess of 20% larger than formula (6) used by Prandtl and Schlichting [1] and Mills and Hang [4]. The average skin-friction coefficient was of minor importance in those works, and wasn't compared with measured data.

Applying formula (41) to the Mills-Hang local formula (3) yields:

$$C_D^2 / C_f \quad (42)$$

For a disrupted boundary-layer the transform for local friction  $f_c$  given average friction  $f_C$  is:

$$\frac{f_c(x)}{f_C(x)} = \left( \frac{d((x - x_S) f_C(x)) / dx}{f_C(x)} \right)^2 \quad (43)$$

Applying formula (43) to the present work's average skin-friction formula (20) produces a formula for local skin-friction coefficient where  $x_S = L_P/\varepsilon$  and  $x_S \leq x \leq L/\varepsilon$ :

$$f_c(x) = \frac{(\ln x + 2(x_S/x - 1))^2}{3 \ln^4 x} \quad \frac{L}{\varepsilon} \geq x > x_S = \frac{L_P}{\varepsilon} \geq 1 \quad (44)$$

The local skin-friction coefficient for smooth turbulent flow can be derived from equations (24) and (45) with  $\text{Re}_x \geq \text{Re}_S \geq \sqrt{3}e$ :

$$\frac{dW_0(z)}{dz} = \frac{W_0(z)}{z(W_0(z) + 1)} \quad f_{c\sigma}(\text{Re}_x) = \frac{d((\text{Re}_x - \text{Re}_S) f_{C\sigma}(\text{Re}_x))}{d\text{Re}_x} \quad (45)$$

$$f_{c\sigma}(\text{Re}_x) = \frac{\sqrt[3]{2} W_0^2(\text{Re}_x/\sqrt{3}) - 2(1 - \text{Re}_S/\text{Re}_x) W_0(\text{Re}_x/\sqrt{3}) - 1}{3 (W_0(\text{Re}_x/\sqrt{3}) - 1)^3 (W_0(\text{Re}_x/\sqrt{3}) + 1)} \quad (46)$$

## 12. Forced convection

The Chilton-Colburn analogy (47) relates friction factors to turbulent forced convective heat transfer, expressed as the average Nusselt number ( $\overline{\text{Nu}}$ ), in terms of  $\text{Re}$  and the fluid's Prandtl number ( $\text{Pr}$ ).

$$\overline{\text{Nu}} = \frac{f_C}{2} \text{Re Pr}^{1/3} \quad (47)$$

Combining equation (47) with equation (20) produces a formula for rough turbulent forced convection:

$$\overline{\text{Nu}} = \frac{\text{Re Pr}^{1/3}}{6 \ln^2(L/\varepsilon)} \quad \frac{L}{\varepsilon} \gg 1 \quad (48)$$

Lienhard [14] finds that there are fluids for which equation (47) is incorrect for smooth turbulence. Convection experiments will test whether it is correct for rough turbulence.

### 13. Experimental results

What can be learned from physical measurements of skin-friction or forced-convection from rough plates?

If measurements of plates with isotropic self-similar roughness were close to the predictions of skin-friction equation (20) or convection equation (48), then those measurements would support the present formulas for self-similar roughness only. If measurements (over a range of  $Re$  values) of diverse plates with periodic isotropic roughness were close to the present predictions, then that would be compelling evidence that the present formulas reflect a physical law of turbulent flow along isotropic surface roughness.

The Convection Machine [15] bi-level plate surface was composed of (676) square  $8.28 \text{ mm} \times 8.28 \text{ mm} \times 6 \text{ mm}$  posts spaced on  $11.7 \text{ mm}$  centers over a  $0.305 \text{ m}$  square plate. The area of the top of each post was  $0.686 \text{ cm}^2$ , half of its  $1.37 \text{ cm}^2$  cell. The RMS height-of-roughness and also the arithmetic-mean height-of-roughness were  $3 \text{ mm}$ . A periodic equal-area bi-level architecture provides the largest RMS height-of-roughness possible in a  $6 \text{ mm}$  peak-to-valley span. This surface has no self-similarity.

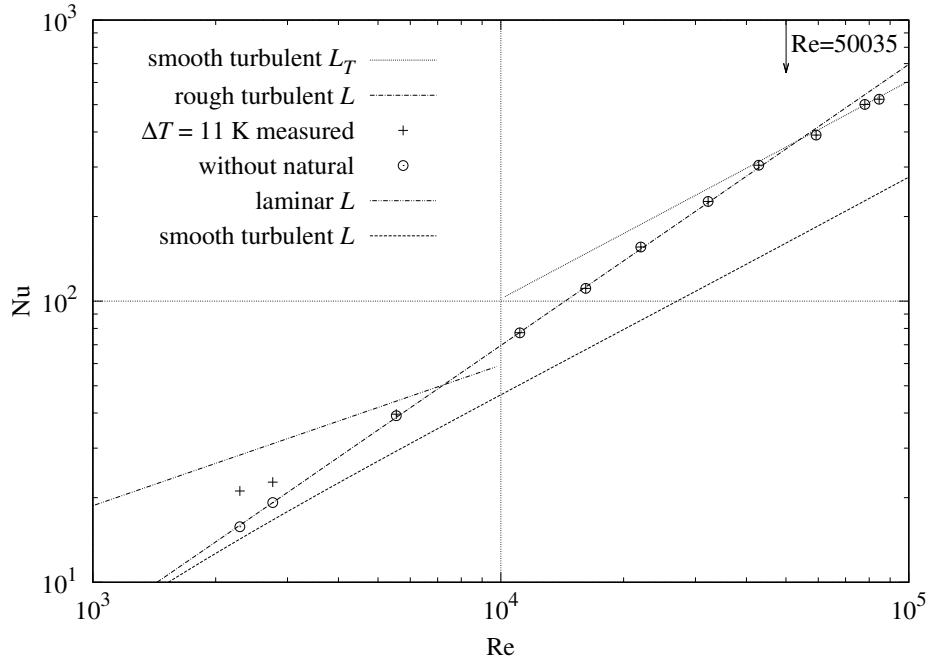


**Figure 14 Convection from rough plate;  $\varepsilon = 3 \text{ mm}$ ;  $L = 0.305 \text{ m}$**

The points labeled “ $\Delta T = 11 \text{ K}$  measured” are the measured  $\overline{Nu}$  values in Figure 14; the points labeled “without natural” discount the natural convection from the measured values using the mixed convection model described in Jaffer [16].

Applying convection formula (48) to the bi-level plate geometry yields  $\overline{Nu} = 0.0078 \text{ RePr}^{1/3}$ . The corresponding trace “rough turbulent  $L$ ” in Figure 14 matches the “without natural” points  $\pm 2\%$  for  $2300 < \text{Re} < 50000$ .

At  $\text{Re} > 50000$  the “smooth turbulent  $L_T$ ” trace (having slope  $4/5$ ) shows that convection is from a smooth turbulent flow, but with a smaller characteristic-length ( $L_T \approx 8.2 \text{ mm}$ ) than “smooth turbulent  $L$ ”. The transition at  $\text{Re}_\ell = 50035$  is computed by equation (37). Constraint (39) indicates that flow will transition from rough turbulence to smooth turbulence at  $\text{Re}_x > \text{Re}_\ell = 50035$  if the post surface roughness  $\varepsilon_q < 0.4 \text{ mm}$ .

With  $L_P/\varepsilon < 193$ , formula (34) predicts that flow over the whole plate transitions directly from laminar to rough turbulence at  $\text{Re}_\lambda \approx 175$ , too small to test directly in the Convection Machine.

The periodic bi-level plate behaving compatibly with formula (48), which was derived from an analysis of self-similar roughness, supports the claim that formulas (20) and (48) are intrinsic to turbulent flow along isotropic roughness and not specific to self-similar roughness.

## 14. Fully rough regime

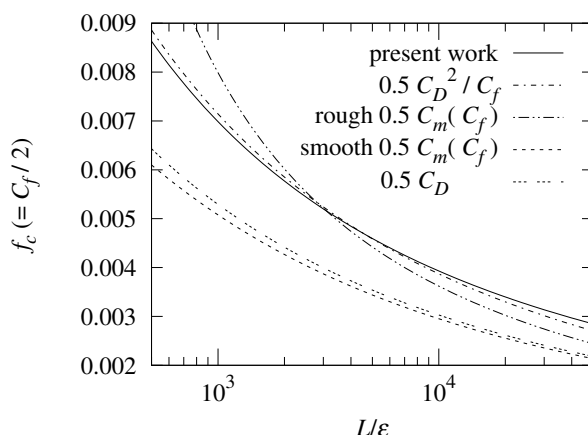


**Figure 15** average friction coefficient of sphere-roughened plate

Figure 15 compares average skin-friction formulas. “ $0.5 C_D$ ” is the Mills-Hang formula (4); “ $0.5 C_m(C_f)$ ” are the Churchill rough and smooth formulas (7); “ $0.5 C_D^2/C_f$ ” is from formula (42). “ $0.5 C_D^2/C_f$ ” is within  $\pm 2.5\%$  of “present work” equation (20) over Mills-Hang’s range  $750 < L/k_S < 2750$  ( $4000 < L/\epsilon < 14650$ ).

This close match in the completely rough regime supports the present theory with the measurements from Pimenta et al [3] as modeled by Mills and Hang [4].

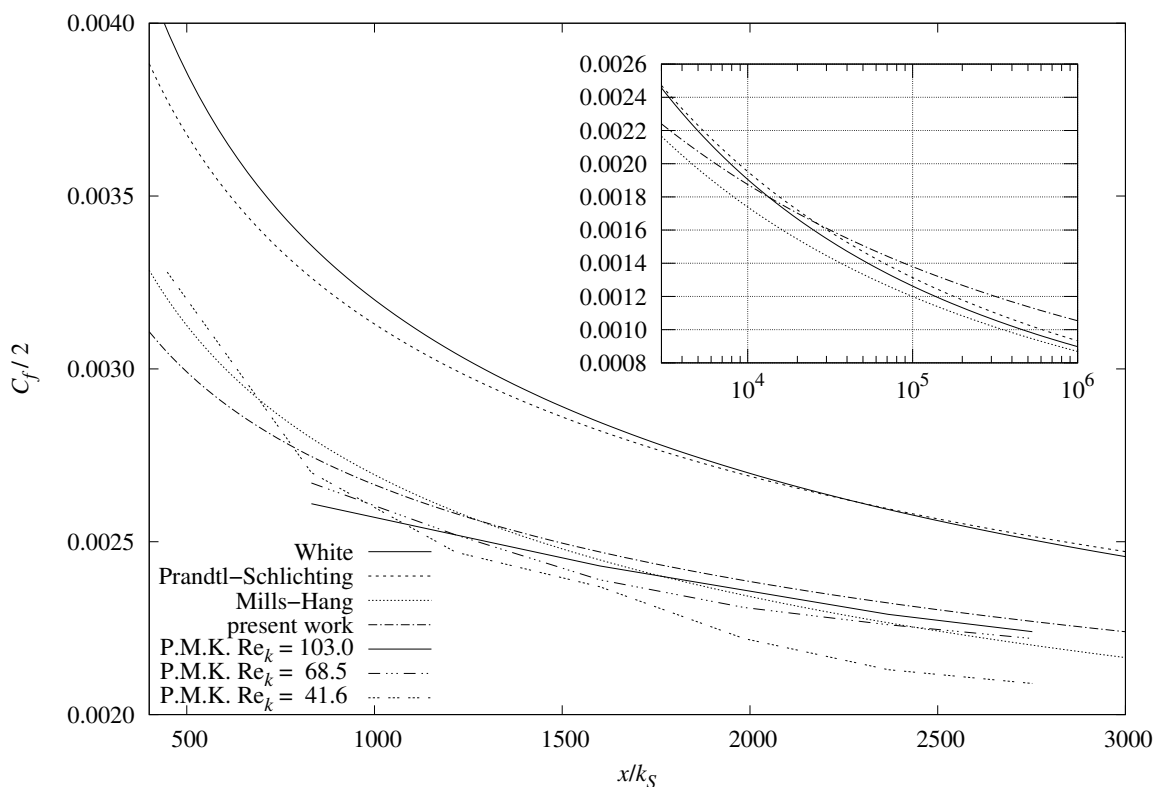


**Figure 16** local skin-friction coefficient

Figure 16 plots the local skin-friction coefficients from Prandtl-Schlichting (1), Mills-Hang (3), White (5) and the present theory (44) in the fully rough regime (large  $Re$ ).

At large  $x/k_S$  the inset graph in Figure 16 shows that the local formulas from Mills-Hang, Prandtl-Schlichting, and White differ from the present work, growing to  $-8\%$ ,  $-13\%$ , and  $-16\%$  relative to  $f_c$  formula (44) at  $L/k_S = 10^6$ . Note that only Prandtl-Schlichting included such a high ratio in their range.

## 15. Transitional rough regime

Afzal, Seena, and Bushra [8] (also Schlichting [5]) relate that the turbulent flow inside commercial pipes behaves differently from the flow inside Nikuradse’s sand coated pipes in the transitional rough regime. While the skin-friction coefficients for commercial pipes are monotonically decreasing with increasing Re on the Moody diagram ( $f_C$  versus Re), in the diagram for Nikuradse’s pipes the coefficient trace for each roughness reaches its minimum just to the right of the smooth skin-friction line, a behavior they term “inflectional”.

The Prandtl-Schlichting plate model inherited the inflectional curve from Nikuradse’s pipes. The average coefficient of resistance ( $c_f$ ) Moody diagram from Prandtl and Schlichting [1] (also Schlichting [5]) shows  $c_f$  following a  $-1/5$  slope smooth turbulent line to a 7% dip spread over a decade of Re just to the right of the smooth turbulent line before leveling out further to the right. An inflectional curve is shown in Figure 17.

The present work’s local and average skin-friction formulas (44) and (20) predict no variation in  $f_c$  with Re from a periodic roughness producing rough turbulence ( $\max(\text{Re}_\lambda, \text{Re}_\sigma) < \text{Re} < \text{Re}_\ell$ ).

The rough surface tested by Pimenta et al [3] was 11 layers of densely packed metal balls 1.27 mm in diameter “arranged such that the surface has a regular array of hemispherical roughness elements.” They used sand-roughness  $k_S = 0.79$  mm.

Being repeating patterns, both sphere-roughened and sand-roughened surfaces are not self-similar.

Prandtl and Schlichting put the boundary between the transitional rough and fully rough regimes for a plate at sand-roughness Reynolds number  $\text{Re}_k = v^* k_S / \nu = 70.8$  where  $v^*$  is the friction velocity from equations (19) and  $\nu$  is the fluid kinematic viscosity. Pimenta et al assign  $\text{Re}_k = 65$ . Solving for Re:

$$\text{Re}_k = v^* k / \nu = \frac{v}{\sqrt{3} \ln(L/\varepsilon)} \frac{5.333 \varepsilon}{\nu} = \frac{5.333 \text{Re}}{\sqrt{3} [L/\varepsilon] \ln(L/\varepsilon)} \quad (49)$$

$$\text{Re} \approx 0.325 \text{Re}_k \frac{L}{\varepsilon} \ln \frac{L}{\varepsilon} \quad (50)$$

Figure 16 shows the local skin-friction coefficient versus  $x/k_S$  for the Pimenta et al sphere-roughened plate at three rates of flow,  $\text{Re}_k = 41.6, 68.5,$  and  $103$ . The averages of these local coefficients<sup>3</sup> (from  $450 < x/k_S < 2800$ ) are 0.00247, 0.00252, and 0.00253 respectively. These averages are within 2.5% of each other, less than the 5% spread predicted by Prandtl and Schlichting. The “Mills-Hang” trace is the fully rough local  $C_f/2$ ; its close proximity to the “P.M.K” traces shows the lack of significant behavioral difference between the regimes.

Figure 17 is a Moody diagram of the 3 mm and 1 mm RMS roughness bi-level plate measurements, with natural convection discounted (as was done for Figure 14), then converted to friction coefficients  $f_C$  using the Chilton-Colburn analogy (47). Only measurements for  $\text{Re} < \text{Re}_\ell$  are shown. The vertical arrows show the Prandtl-Schlichting and Pimenta et al regime boundaries calculated for 3 mm RMS roughness by equation (50). The  $L/k_S = 19.1$  trace is the  $c_f = 0.0320$  value calculated by Prandtl-Schlichting formula (2) for 3 mm RMS roughness. Pimenta et al [3] and Mills and Hang [4] use  $c_f/2$  in order to bring its value into proximity with measurements.

An assumption of pipe analogy theories is that rough skin-friction coefficients will not be less than smooth turbulent coefficients  $f_{C\sigma}$  in all turbulent flow regimes. Note that using  $c_f/2$  instead of  $c_f$  (while leaving  $f_{C\sigma}$  unchanged) violates that assumption.

The “measured” points in Figure 17 are within 2% of the “ $L/\varepsilon = 102$ ” line at  $f_C \approx 0.0156$ . The points follow neither an “inflectional” nor “monotonic” trajectory. And clearly, some coefficients are less than  $f_{C\sigma}$ . The point near “ $L/\varepsilon = 305$ ” shows that  $f_C$  can be less than  $f_{C\sigma}$ , even at Re values a decade smaller than the smooth turbulent intercept (although it is much closer to  $f_C = 0.0102$  than its  $\pm 7\%$  expected measurement uncertainty).

---

<sup>3</sup>  $C_f/2$  at  $x/k_S = 452$  was measured only at  $\text{Re}_k = 41.6$ ; it is included in all three averages.

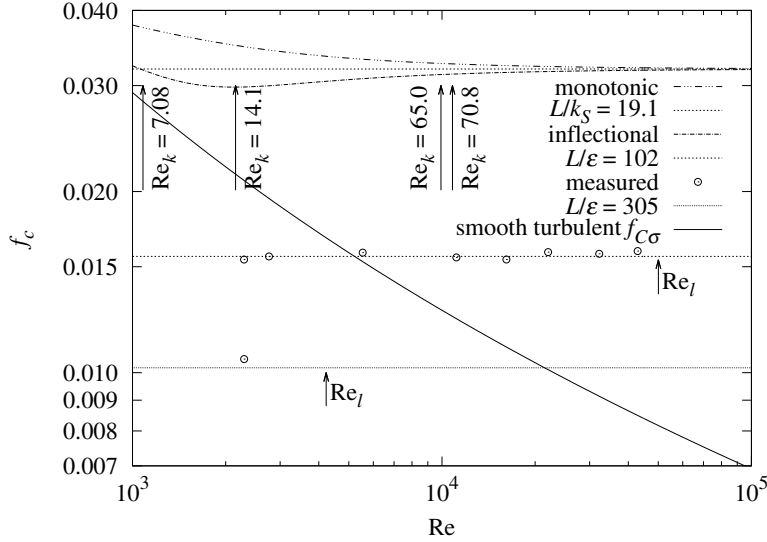


Figure 17 average  $f_C$  versus  $Re$  of bi-level plate

## 16. Discussion

Recapping the development:

- In rough turbulence the surface roughness disrupts boundary layer flow over a plate.
- Self-similar roughness has a constant characteristic-length to RMS height-of-roughness ratio  $L/\epsilon \gg 1$  at a succession of scales converging to zero.
- Flat surfaces with isotropic self-similar roughness have skin-friction coefficients dependent only on  $L/\epsilon$ :  $f_C = (1/3) \ln^{-2}(L/\epsilon)$
- Consideration of the roughness  $Re$  at high  $L/\epsilon$  leads to an exact formula for the turbulent skin-friction coefficient for a smooth plate:  $f_{C\sigma} = (\sqrt[3]{2}/3) (W_0 (Re/\sqrt{3}) - 1)^{-2}$
- This smooth-turbulent formula matches measurements from Smith and Walker (1959) and Spalding and Chi (1964) within  $\pm 0.75\%$ .
- Periodic roughness is not self-similar. The effective period  $L_P = L/j_P$ , where  $j_P \gg 1$  is the index of the discrete Fourier transform coefficient  $X_j$  with the largest amplitude.
- Experiments with periodic isotropic roughness (bi-level and sphere-roughened plates) find that the average (not local) skin-friction coefficient is within  $\pm 2.5\%$  of  $f_C$  over wide ranges of  $Re$ . That flows from such dissimilar rough surfaces hew so closely to the present formulas is compelling evidence that these formulas reflect physical laws of turbulent flow along isotropic surface roughness.
- The transition from laminar or smooth turbulent flow to rough turbulent flow along a plate with isotropic periodic roughness occurs when  $\epsilon$  exceeds the larger of the local (laminar or smooth turbulent) momentum thicknesses of a smooth plate at  $x = L_P$ .
- When  $L_P/\epsilon < 193$  the flow over the whole plate transitions from laminar flow to rough turbulence at  $Re_\lambda$ .
- This transition to rough turbulence is an order of magnitude lower than predicted by pipe analogy theories.  $f_C$  is constant above  $Re_\lambda$  (and below  $Re_\ell$ );  $f_C$  measurements of the bi-level plate are flat within 2% through the boundaries between hydraulically smooth, transitional, and fully rough regimes of pipe analogy theories.
- Downstream from a disruption, a turbulent boundary layer restarts from zero thickness over a flat, smooth patch. If this boundary layer grows large enough to bridge the rough bits outside of the smooth patches, then the flow downstream will be smooth turbulent. A formula for this threshold  $Re_\ell$  was developed; the convection model using it matches the measurements for the 1 mm and 3 mm roughness bi-level plates within their expected measurement uncertainties.
- Comparison of the present theory with both local and average measurements shows good agreement through all the turbulent regimes.

Self-similar roughness disrupts emerging boundary layers along its entire length, generating the most turbulence (as revealed by its skin-friction coefficient) possible from a given height-of-roughness. Periodic roughness generates the same amount of turbulence for  $\max(\text{Re}_\lambda, \text{Re}_\sigma) < \text{Re} < \text{Re}_\ell$ .

The present work finds that rough turbulence over a plate is a simpler phenomena than smooth turbulent flow. Rough turbulent flow has a constant skin-friction coefficient dependent only on the ratio of characteristic-length to RMS height-of-roughness.

Equation (47) is the original (1933) form of the Chilton-Colburn analogy. Lienhard [14] demonstrates that these particular Re and Pr exponents are not correct for smooth turbulent flow in all fluids. In particular, the Pr exponent should be 0.6 in gasses. The present theory matches rough turbulent convection on the Convection Machine within its  $\pm 2\%$  expected measurement uncertainty using  $\text{Pr}^{1/3}$ . With  $\text{Pr} = 0.71$  (for air),  $\text{Pr}^{0.6}$  is nearly 9% larger than  $\text{Pr}^{1/3}$ , far exceeding the  $\pm 2\%$  expected measurement uncertainty.

This  $\text{Pr}^{1/3}$  form of the analogy is consistent with rough turbulence's repeated boundary-layer disruptions being less dependent on fluid properties (not captured by  $\text{Pr}^{1/3}$ ) than is the generation of smooth turbulence.

For periodic isotropic roughness, the  $L \gg L_P$  condition guarantees that the transition to rough turbulence occurs in the leading band of periodic roughness, which controls the flow over the rest of the plate. When  $L_P/\varepsilon > 194$ ,  $\text{Re}_\lambda$  is the "critical Re".

The smooth turbulent threshold  $\text{Re}_\sigma < 1$  for both bi-level plates and the rough surface tested by Pimenta et al. The laminar threshold  $\text{Re}_\lambda \approx 1577$  for the  $\varepsilon = 1$  mm bi-level plate.  $\text{Re} = 1577$  is too slow to test in the Convection Machine wind-tunnel. For a bi-level plate having 0.5 mm height-of-roughness  $\text{Re}_\lambda = 6310$ , but free-stream turbulence of the wind-tunnel might still prevent laminar flow.

## 17. Conclusions

- The turbulent skin-friction coefficient for a smooth plate is:

$$f_{C\sigma} = \frac{\sqrt[3]{2}}{3} \ln^{-2} \left( \frac{\exp(W_0(\text{Re}/\sqrt{3}))}{e} \right) = \frac{\sqrt[3]{2}/3}{[W_0(\text{Re}/\sqrt{3}) - 1]^2} \quad \text{Re} \gg \sqrt{3}e$$

where  $W_0$  is the smallest positive branch of the Lambert  $W$  function, the inverse of  $x \exp x$ .

- For a plate surface with periodic or self-similar isotropic RMS height-of-roughness  $\varepsilon > 0$ , which is producing rough turbulence in a steady flow of strength Re, the average skin-friction coefficient and forced convection formulas are:

$$f_C = \frac{1}{3 \ln^2(L/\varepsilon)} \quad \overline{\text{Nu}} = \frac{\text{Re} \text{Pr}^{1/3}}{6 \ln^2(L/\varepsilon)} \quad \frac{L}{\varepsilon} \gg 1$$

- For periodic isotropic roughness with period  $L_P \ll L$ , when  $L_P/\varepsilon < 193$ , the flow over the whole plate transitions directly from laminar to rough turbulence at  $\text{Re}_\lambda$ . When  $L_P/\varepsilon > 194$ , then  $\text{Re}_\sigma > \text{Re}_\lambda$  and the flow over the whole plate transitions from laminar to smooth turbulence at  $\text{Re}_\lambda$ , and to rough turbulence at  $\text{Re}_\sigma$ .

$$\text{Re}_\lambda = \left( \frac{0.664}{\varepsilon} \right)^2 L_P L \quad \text{Re}_\sigma = \left( \frac{0.036}{\varepsilon} \right)^5 L_P^4 L$$

- For periodic isotropic roughness with period  $L_P \ll L$  and flat patches in each cell with length  $L_T < L_P$  in the direction of flow, patch roughness  $\varepsilon_q \ll \varepsilon$ , and patch period  $L_q < L_T$ , the flow will be rough turbulent (to which the formulas apply) when  $\text{Re} > \max(\text{Re}_\lambda, \text{Re}_\sigma)$  and:

$$\text{Re}_x < \text{Re}_\ell = \frac{L/8}{0.036 L_T} \left( \frac{2\varepsilon}{0.036 L_P} \right)^{9/4} < \frac{L}{L_q} \left( \frac{0.036 L_q}{\varepsilon_q} \right)^5$$

## 18. Nomenclature

	$\overline{\text{Nu}}$ = average Nusselt number (convection)
	$\text{Pr}$ = fluid Prandtl number
	$\text{Re}$ = Reynolds number of flow parallel to the plate
	$\text{Re}_\ell$ = local Re rough-to-smooth turbulence threshold
$\text{Re}_\varepsilon = v^* \varepsilon / \nu, \text{Re}_k = v^* k_S / \nu$	= roughness, sand-roughness Reynolds number
	$\text{Re}_\lambda$ = laminar Reynolds number upper-bound
	$\text{Re}_\sigma$ = smooth turbulent Reynolds number upper-bound
$\text{Re}_x = x \text{Re} / L$	= local Reynolds number
	$C_f, C_D$ = Mills-Hang local, average friction coefficient
	$C_m$ = Churchill mean (average) friction coefficient
	$C_f/2$ = Pimenta et al local friction coefficient
	$c'_f, c_f$ = Prandtl-Schlichting local, average friction coefficient
	$f_c, f_C$ = local, average friction coefficient
	$G(x, w)$ = Gray-code profile function
	$j_P$ = index of largest $X_j$
	$k_S$ = sand-roughness (m)
	$L$ = plate characteristic-length (m)
	$L_P$ = effective roughness period (m)
	$L_q$ = smooth patch roughness period (m)
	$L_T$ = average periodic flat length in direction of flow (m)
	$n$ = branching factor of profile roughness function
	$S_j$ = compensated discrete Fourier transform coefficient
	$v$ = bulk fluid (= free-stream) velocity (m/s)
	$v^*$ = friction velocity (m/s)
	$w = 2^t$ = integer power of two
	$W_0$ = smallest positive branch of the Lambert $W$ function
	$W(x, w)$ = wiggliest integer self-similar profile
	$Y(x, w)$ = integer ramp-permutation self-similar profile
	$X_j$ = discrete Fourier transform coefficient
	$x, y$ = distance (m)
	$z(x)$ = profile roughness function (m)
	$\bar{z}$ = mean height of roughness (m)
	$Z$ = profile roughness function random variable (m)

## Greek Symbols

	$\delta_2$ = momentum thickness of boundary-layer (m)
	$\delta_{2\lambda}$ = momentum thickness, laminar boundary-layer (m)
	$\delta_{2\sigma}$ = momentum thickness, turbulent boundary-layer (m)
	$\epsilon$ = RMS profile height-of-roughness (m)
	$\varepsilon$ = RMS surface height-of-roughness (m)
	$\varepsilon_q$ = periodic smooth patch height-of-roughness (m)
$t = \log_2 w$	= positive integer
	$\nu$ = fluid kinematic viscosity ( $\text{m}^2/\text{s}$ )
	$\rho$ = fluid density ( $\text{kg}/\text{m}^3$ )
	$\tau$ = fluid shear stress ( $\text{N}/\text{m}^2$ )

## Acknowledgments

The idea of self-similar roughness grew out of a discussion with Nina Koch about turbulence self-similarity. Thanks to John Cox and Doug Ruuska for machining the bi-level plates.

Thanks to Martin Jaffer for insight into conversions between local and average skin-friction coefficients.

## 19. References

- [1] L. Prandtl and H. Schlichting. *The Resistance Law for Rough Plates*. Translation (David W. Taylor Model Basin). Navy Department, the David W. Taylor Model Basin, 1934. Translated 1955 by P.S. Granville.
- [2] F. R. Hama. Boundary layer characteristics for smooth and rough surfaces. *Trans. Soc. Nav. Arch. Marine Engrs.*, 62:333–358, 1954.
- [3] M. M. Pimenta, R. J. Moffat, and W. M. Kays. *The Turbulent Boundary Layer: An Experimental Study of the Transport of Momentum and Heat with the Effect of Roughness*. Department of Mechanical Engineering, Stanford University, 1975.
- [4] A. F. Mills and Xu Hang. On the skin friction coefficient for a fully rough flat plate. *J. Fluids Eng*, 105(3):364–365, 1983.
- [5] Hermann Schlichting, Klaus Gersten, Egon Collaborateur. Krause, Herbert Collaborateur. Oertel, and Katherine Mayes. *Boundary-layer theory*. Springer, Berlin, Heidelberg, Paris, 2000. Corrected printing 2003.
- [6] Frank White. *Viscous Fluid Flow, 3rd Edition*. McGraw-Hill, 2006.
- [7] Stuart W. Churchill. Theoretically based expressions in closed form for the local and mean coefficients of skin friction in fully turbulent flow along smooth and rough plates. *International Journal of Heat and Fluid Flow*, 14(3):231 – 239, 1993.
- [8] Noor Afzal, Abu Seena, and A. Bushra. Turbulent flow in a machine honed rough pipe for large reynolds numbers: General roughness scaling laws. *Journal of Hydro-environment Research*, 7(1):81–90, 2013.
- [9] Karen A Flack, Michael P Schultz, Julio M Barros, and Yechan C Kim. Skin-friction behavior in the transitionally-rough regime. *International Journal of Heat and Fluid Flow*, 61:21–30, 2016.
- [10] J.H. Lienhard, IV and J.H. Lienhard, V. *A Heat Transfer Textbook*. Phlogiston Press, Cambridge, MA, 5th edition, 2019. Version 5.00.
- [11] Mitchell G. Newberry and Van M. Savage. Self-similar processes follow a power law in discrete logarithmic space. *Phys. Rev. Lett.*, 122:158303, Apr 2019.
- [12] D. W. Smith and J. D. Walker. Skin friction measurements in incompressible flow. Technical Report R-26, NASA, Washington, DC, 1959.
- [13] D. B. Spalding and S. W. Chi. The drag of a compressible turbulent boundary layer on a smooth flat plate with and without heat transfer. *Journal of Fluid Mechanics*, 18(1):117143, 1964.
- [14] V Lienhard, John H. Heat Transfer in Flat-Plate Boundary Layers: A Correlation for Laminar, Transitional, and Turbulent Flow. *Journal of Heat Transfer*, 142(6), 04 2020. 061805.
- [15] Aubrey Jaffer. Convection measurement apparatus and methodology, 2019. <http://people.csail.mit.edu/jaffer/convect/measure.pdf>.
- [16] Aubrey Jaffer. Turbulent mixed convection from an isothermal plate, 2019. <http://people.csail.mit.edu/jaffer/convect/mixed.pdf>.